

Article

Nanoparticle Number Concentration in the Air in Relation to the Time of the Year and Time of the Day

Jáchym Brzezina ^{1,*}, Klaudia Köbölová ² and Vladimír Adamec ²¹ Air Quality Department, Czech Hydrometeorological Institute, 616 67 Brno, Czech Republic² Institute of Forensic Engineering, Brno University of Technology, 612 00 Brno, Czech Republic; xckobolova@usi.vutbr.cz (K.K.); vladimir.adamec@usi.vutbr.cz (V.A.)

* Correspondence: jachym.brzezina@chmi.cz; Tel.: +420-541421046

Received: 6 May 2020; Accepted: 15 May 2020; Published: 19 May 2020



Abstract: The paper analyzes suspended particles number concentrations of 61 size fractions (184 nm to 17,165 nm) in the air at a traffic location. The average course of the individual fractions was analyzed at various intervals – daily, weekly, monthly and annually, in the period between 2017 and 2019. The data was then used to calculate the arithmetic mean for all the fractions (MS Excel, R) and then using a proprietary web application, heatmaps were constructed. The obtained results showed significant differences in both the annual and daily variation of number concentrations between the individual fractions differing in particle size. In the case of the annual variation, one can see a greater variability of smaller particles, which is most likely due to the source of the actual suspended particles. Meteorological and dispersion conditions are found as important factors for suspended particle concentrations. These can lead to significant differences from year to year. However, a comparison between 2018 and 2019 showed that even though the average absolute number concentrations can differ between years, the actual relative number concentrations, i.e., the ratios between the individual fractions remain very similar. In conclusion it can be said that the difference between the number concentration variation of the size fractions depends on both the actual pollution sources (especially in the long-term, i.e., the annual variation) and the actual size of the particles, which plays a role especially in the short-term (daily, weekly variation).

Keywords: PM pollution; seasonality; air quality; meteorological conditions

1. Introduction

Air pollution has recently been identified as a major issue in the field of the environment and public health [1]. Suspended particles (PM) can potentially have very undesirable effects on human health [2]. These particles are suspended in the atmosphere and can have a very complex chemical composition and have variable sizes. Sources of fine particles (aerodynamic diameter of $<2.5 \mu\text{m}$) and ultrafine particles (aerodynamic diameter of $<0.1 \mu\text{m}$) include both natural and anthropogenic sources [3]. The increase in concentrations of $\text{PM}_{2.5}$ and $\text{PM}_{0.1}$ has recently become a global issue due to their impact on human health, air pollution and the atmospheric and climate system [4–6]. In general, the smaller the particle, the potentially more dangerous it is for human health as it penetrates deeper into the respiratory system or even directly to the bloodstream in the case of the smallest nanoparticles.

The current legislation in the Czech Republic and European Union as a whole specifies only mass concentrations of particles $\text{PM}_{2.5}$ and PM_{10} (aerodynamic diameter $<10 \mu\text{m}$). However, in an urban environment, the ultrafine particles represent more than 90% of particles in terms of their overall count (number concentration), but their mass concentration is negligible in comparison to large particles. There is no exact regulation for air pollution in terms of the PM_1 fraction [7,8]. This gap in legislation is due to insufficient data available for the PM_1 effects on the environment and human

health, because measuring smaller particles is demanding financially and technically. Nanotoxicological studies, however, show that particles in the nano range have completely different physio-chemical properties such as lower weight, ultrahigh reactivity, a high ratio between surface area and mass etc. These unique properties can pose more serious consequences for human health compared to particles of a larger size. It is therefore very important to study the PM_1 and $PM_{0.1}$ particles and measure and characterize their concentration and distribution [9,10].

Lots of information and studies are available for the PM_{10} and partially also the $PM_{2.5}$ particles in Europe [11–13], however, data for the PM_1 particles, especially regarding their chemical composition and concentrations [14–16], short-term measurements [17–19] or long term measurements [20–22] are still insufficient.

Significant changes in seasonal variability have been observed for the concentration and size distribution of ultrafine particles. Samek et al. analyzed the seasonality effect on fine and ultrafine particles from various sources. These included combustion processes (fossil fuels, biomass), secondary aerosols, and the category “other”, which included traffic, industry and soil. In winter, the major sources were combustion and secondary aerosols. In the case of combustion, fine particles dominated (53% by mass for $PM_{2.5}$), while ultrafine particles represented 27%. Secondary aerosols in winter were composed of especially PM_1 (approximately 63%). In summer, the contribution from combustion was much smaller, from 3% to 6%. The contribution of secondary aerosols in the summer was approximately 50% for both fractions. The average particle concentration in summer months for PM_1 was $16.4 \pm 8.3 \mu\text{g}\cdot\text{m}^{-3}$ and for $PM_{2.5}$ it was $27.2 \pm 14.1 \mu\text{g}\cdot\text{m}^{-3}$. In winter months the concentrations increased to $58.0 \pm 18.4 \mu\text{g}\cdot\text{m}^{-3}$ for PM_1 and $58.6 \pm 29.5 \mu\text{g}\cdot\text{m}^{-3}$ for $PM_{2.5}$ [17]. Similar correlations between seasons and PM concentrations has also been proved by other studies [23–25].

Some studies studied the effect of traffic on particle number concentration in different seasons of the year. Meteorology and traffic emissions play a significant role in urban air quality, but relationships among them are very complicated [26,27]. Dédelé et al. [28] tried to estimate the inter-seasonal differences in concentration of PM_{10} at different site types. The highest mean concentration of PM_{10} was determined at sites classified as urban background in the winter season ($34.8 \mu\text{g}/\text{m}^3$), while in spring and summer, the highest concentrations of PM_{10} were determined at traffic sites, which were characterized by high traffic intensity (>10,000 vehicles per day). This is a result of the low level of emissions from domestic heating during the warm period of the year, which means that vehicle emissions contribute more to the overall concentrations. The mean PM_{10} concentrations measured at traffic sites ranged from $20.4 \mu\text{g}/\text{m}^3$ in summer to $41.8 \mu\text{g}/\text{m}^3$ in the winter season. Kamińska [29] analyzed the relationship between pollution, traffic, and meteorological parameters. As for the $PM_{2.5}$ concentrations, the meteorological conditions had the largest effect. Only in the summer, the significance of traffic intensity was comparable to that of the meteorological conditions. This can again be explained by the low level of emissions from domestic heating in that part of the year. This finding is in accordance with the analyses performed in other cities [30,31].

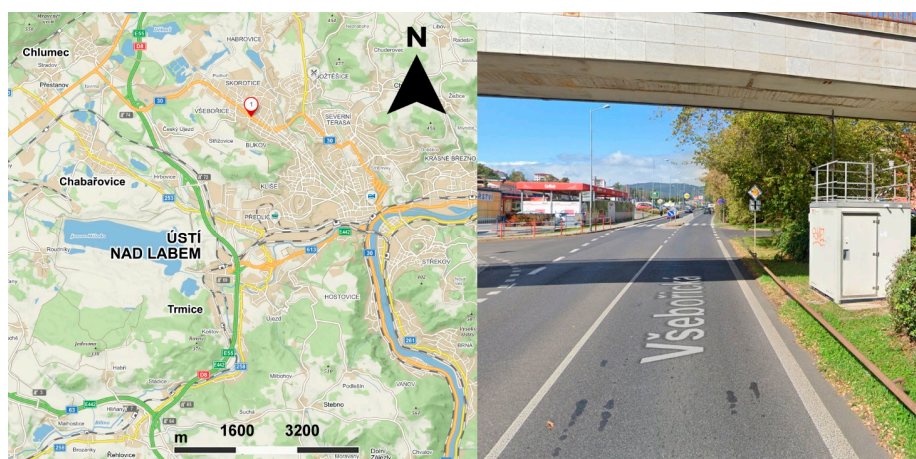
Results presented in this study are based on pilot measurement at the ambient air quality at a monitoring station in Ústí nad Labem, where number concentrations have been measured since mid-2017. The main goal of this analysis was to compare the variation of various size fractions in daily, weekly and annual intervals. The monitored size fractions ranged from approximately 200 nm to particles larger than $15 \mu\text{m}$ in aerodynamic diameter.

2. Experiments

The study used data from continuously measuring automated ambient air quality monitoring station in Ústí nad Labem. The city lies in the northwest of the Czech Republic and is the center of the Ústecký region. The location is in an urban, residential and commercial area. The station is classified as a traffic station as it is located 2 m from a busy road in the direction of Teplice, Prague and Dresden (D8) on the city outskirts. Local domestic heating is an important source of pollution in this location as well. A more detailed characterization of the location is provided in Table 1 and in Figure 1.

Table 1. Characterization of ambient air quality monitoring station Ústí nad Labem-Všebořická.

Basic Characterization	
Station ID	UULD
Name	Ústí nad Labem – Všebořická (hot spot)
Country	Czech Republic
Region	Ústecký
District	Ústí nad Labem
Classification	
Abbreviation	T/U/RC
EOI – station type	traffic (T)
EOI – zone type	urban (U)
EOI B/R – zone characteristic	Residential, commercial (RC)
Location	
Geographic co-ordinates	50°40′59.248″ N 13°59′52.344″ E
Elevation	230 m
Further Details	
Terrain	Flat
Landscape	Multistory housing development
Representativeness	100–500 m

**Figure 1.** Photograph of the ambient air quality monitoring station Ústí nad Labem-Všebořická [32,33].

The station is located in the city of Ústí nad Labem near the Všebořická street. It is labeled as a “hot spot” station meaning it is primarily focused on air pollution from traffic. The station is equipped with the Pallas Fidas 200 analyzer (see Table 2), which works in an automated measuring mode including measurements of particle count distribution. The analyzed particles range from 180 nm to 100 µm in aerodynamic diameter and the measuring range is 0–20,000/cm³. Volume flow is 4.8 L/min (0.3 m³/h). The measurement is based on optical light-scattering. Measurement includes monitoring of PM₁, PM_{2.5}, PM₁₀ and TSP concentrations, and particle size distribution. This measurement is set to monitor over 60 different particle-size fractions. Data used in this study included the period from 15 June 2017 to 31 December 2019 with an interval of measurement of 10 min. The station is also equipped with a traffic counter. In the period of analysis, the average daily car count was 16,751. The majority of the traffic represented passenger cars (79.99%), then vans (12.15%). Large goods vehicles represented 3.87% and large trucks 3.99%.

Table 2. Specification of the Pallas Fidas 200 analyzer.

Measurement Range (Size)	0.18–100 μm (3 Measuring Ranges)
Size channels	64 (32/decade)
Measuring principle	Optical light-scattering
Measurement range (number CN)	0–20,000 particles/cm ³
Time resolution	1 s - 24 h, 15 min in type approved operation
Volume flow	4.8 L/min \pm 0.3 m ³ /h
Data acquisition	Digital, 20 MHz processor, 256 raw data channels
Power consumption	Approx. 200 W
User interface	Touchscreen, 800 \times 480 Pixel, 7"
Power supply	115–230 V, 50–60 Hz
Housing	Table housing, optionally with mounting brackets for rack-mounting
Dimensions	450 \times 320 \times 180.5 mm (H \times W \times D), 19"
Software	PDAnalyze Fidas [®]
Aerosol conditioning	Thermal with IADS
Measurement range (mass)	0–10,000 $\mu\text{g}/\text{m}^3$
Reported data	PM ₁ , PM _{2.5} , PM ₄ , PM ₁₀ , TSP, CN, particle size distribution, pressure, temperature, humidity
Sampling head	Sigma-2

3. Results

The period of analysis represented the period from 15 June 2017 to 31 December 2019. Particle number concentrations per cm³ were monitored in 61 fractions (from 184 nm up to larger than 17,165 μm , see Table 3) in 10-min intervals. The analysis was focused on the average course of the individual fractions for various time intervals – daily, weekly, and annual variations.

Table 3. Monitored size fractions.

Fraction (nm)	Fraction (nm)	Fraction (nm)	Fraction (nm)
184–198	583–627	2130–2289	7239–7779
198–213	627–674	2289–2460	7779–8359
213–229	674–724	2460–2643	8359–8983
229–246	724–778	2643–2841	8983–9653
246–264	778–836	2841–3053	9653–10,373
164–284	836–898	3053–3280	10,373–11,147
284–305	898–965	3280–3525	11,147–11,979
305–328	965–1037	3525–3788	11,979–12,872
328–352	1037–1198	3788–4071	12,872–13,833
352–379	1198–1383	4071–4374	13,833–14,865
379–407	1383–1486	4374–4701	14,865–15,974
407–437	1486–1597	4701–5051	15,974–17,165
437–470	1597–1717	5051–5833	>17,165
470–505	1717–1845	5833–6268	
505–543	1845–1982	6268–6736	
543–583	1982–2130	6736–7239	

To compare the differences between the individual fractions, the absolute number concentrations of the individual fractions have been converted to relative values, where the overall arithmetic mean

for each fraction has been calculated and the value from each interval (hour, day of the week, month) has been related to this mean value.

The following heatmap (Figure 2) shows the differences in variation of the individual fractions. The X-axis represents the individual size fractions, the Y-axis represents the hours of the day. Data are shown as a relative value of each hour to the overall arithmetic mean of that particular size fraction. The visualization clearly shows that fractions of smaller particles have two obvious peaks correlating with traffic peaks in the morning and in the afternoon. However, larger particles (approximately $>1.5 \mu\text{m}$) show an increase during the day, where the number concentration increases during the morning peak hours and do not go down significantly until the end of the afternoon peak hour. One can also see that the number concentration drops much more significantly during the night in the case of the larger particles. One can, therefore, say that the variability is greater in case of the larger particles. While the 213–229 nm fraction only has a difference between the minimum and the maximum ratio of the individual hours of 0.17, the larger fractions have a difference of even more than 1 (9653–10,373 nm – 1.06; 15,976–17,165 nm – 1.09; $>17,165$ nm – 1.18).

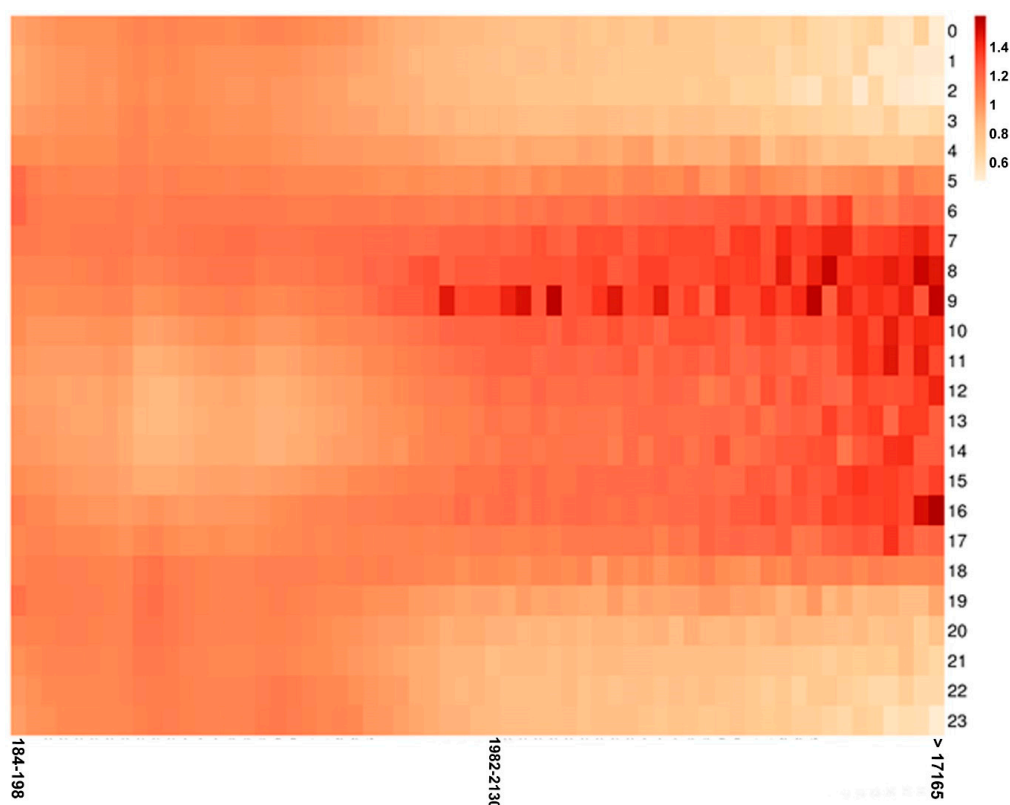


Figure 2. Heatmap showing daily variation (hourly average, Y-axis) of all the size fractions (X-axis, in nm) analyzed.

Similarly to the hourly averages, ratios between average number concentrations for weekdays (Monday–Friday) and weekends (Saturday–Sunday) have been calculated for the individual fractions (Figure 3), where the ratio corresponds to the average number concentration of that fraction on the weekend (Saturday–Sunday) divided by the average number concentration of that fraction on weekday (Monday–Friday). The graph clearly shows that the difference between weekdays and weekends is least profound in the case of the smaller fractions around 300 nm, where the ratio between average of weekday and weekend number concentration is close to 1, i.e., same values. In contrast, most significant differences were observed in case of the larger fractions, where the ratio was approximately 0.65 (smallest for 14,865–15,974 nm fraction, 0.642), i.e., the number concentration during the weekend was approximately 65% of those observed during weekdays.

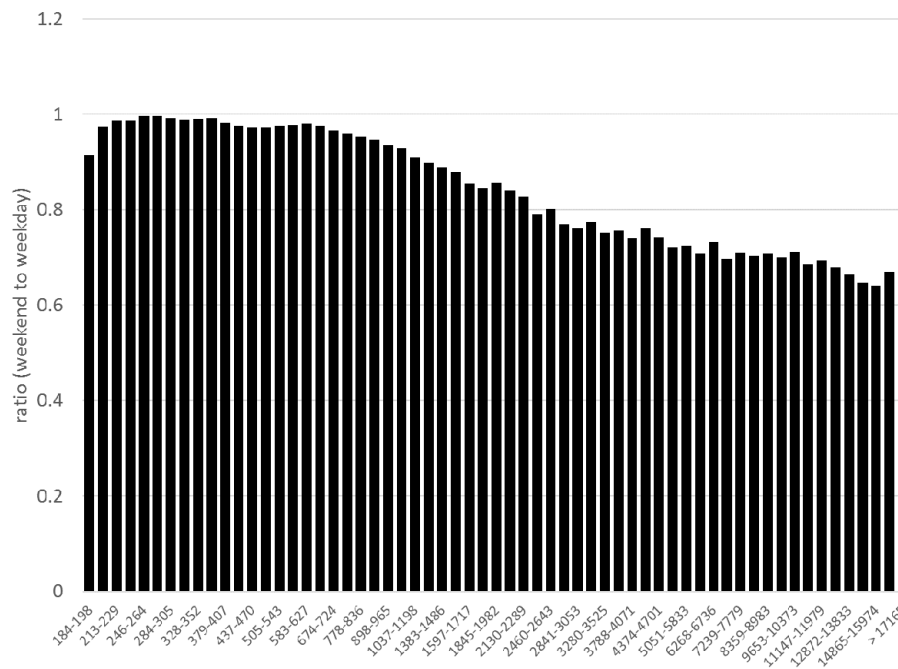


Figure 3. Ratio between average number concentration on the weekdays (Monday-Friday) and the weekends (Saturday-Sunday) weekend/weekday.

Analysis of annual variability was also summarized in a heatmap (Figure 4), where the Y-axis represents the individual months and X-axis the various size fractions. The actual value represents the ratio of the particular monthly mean in relation to the overall mean value of that fraction.

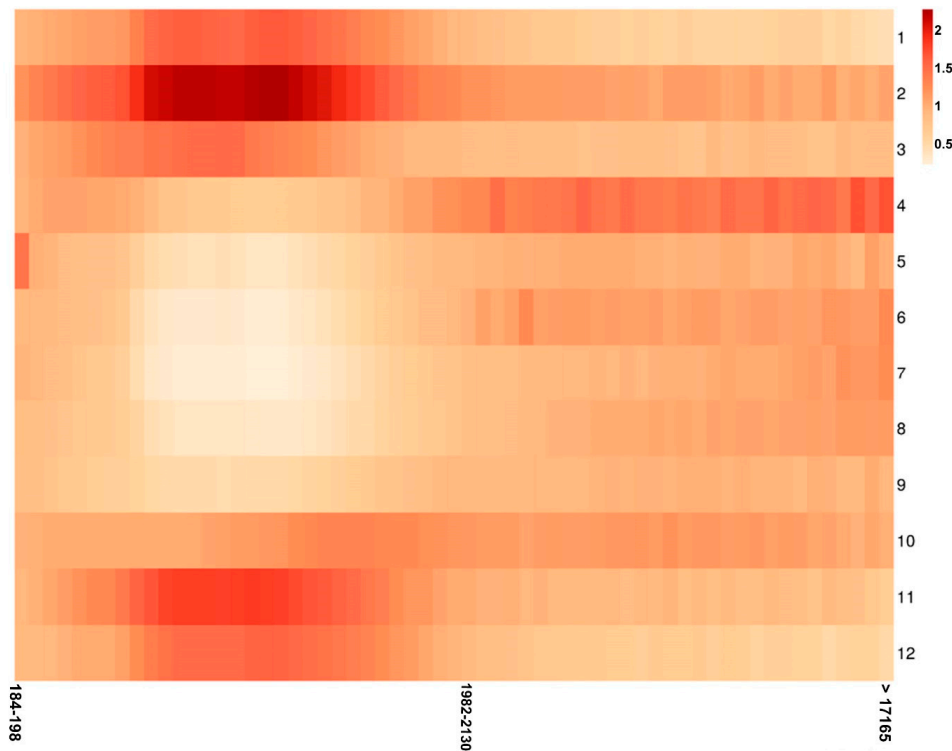


Figure 4. Heatmap showing annual variation (monthly average, Y-axis) of all the size fractions (X-axis, in nm) analyzed.

It can be clearly seen that the number concentrations in the case of the smaller particles were high especially in the winter months. In particular, in the case of particles in the range from 320 to 800 nm. In contrast, larger particles had the average number concentrations distributed throughout the year much more evenly.

If we divide the year into two half-years – cold (October–March) and warm (April–September), we can compare the ratio between the average number concentrations for both these half-years (Figure 5), where the ratio corresponds to the average number concentration of a particular fraction during the cold half-year divided by the average number concentration of a particular fraction during the warm half-year. The graph shows the individual size fractions (X-axis) and the ratio between the cold and warm half-years (Y-axis).

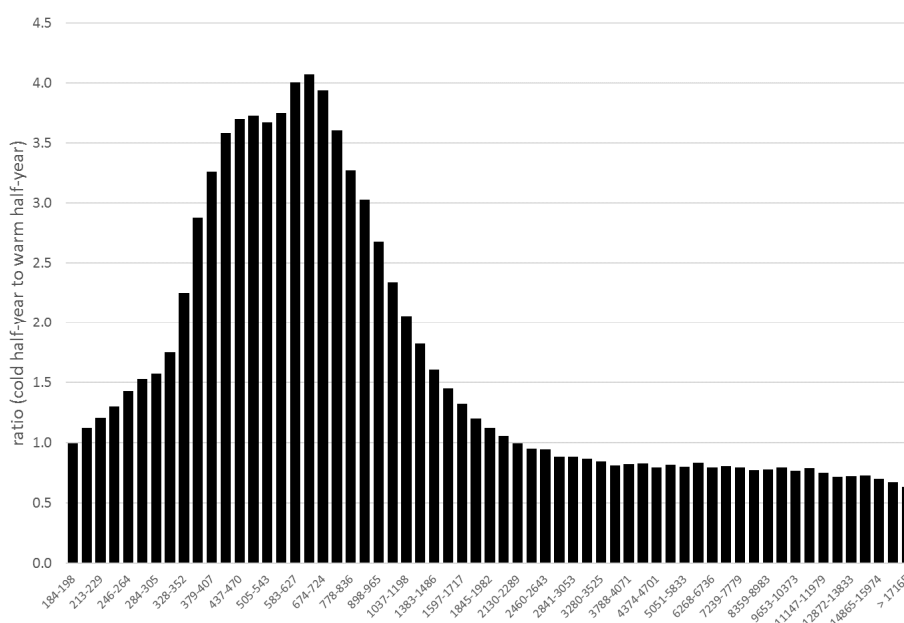


Figure 5. Ratio (Y-axis) between average number concentration of all the size fractions (X-axis) between the cold half-year (October–March) and warm half-year (April–September) (cold half-year/warm half-year).

The trends in the ratio show that the fractions can be divided into three groups – the smallest particles (approximately 180–320 nm), which have similar number concentrations during both half-years, medium-sized particles (approximately 320 to 700 nm) where there is a gradual increase in the relative number concentrations in the winter period, with maximum ratio observed in case of the fraction 627–674 nm (4.07). Then as the particles get larger the ratio decreases. The last group of particles, with an aerodynamic larger than approximately 2 μm, has lower number concentrations in the cold half-year than in the warm half-year. In the case of the fraction >17,165 nm, the ratio is 0.63.

To see how the various years compare a comparison was made between the two complete years 2018 and 2019 (Figure 6), in particular, the average number concentrations of the individual size fractions from the entire year were compared.

It is obvious that the two years differ in terms of the absolute values of the average number concentrations, with higher values in 2018 (most likely due to overall better meteorological and dispersion conditions in 2019, which was a very warm year). If, however, we convert the absolute values to relative ones, i.e., calculate the relative ratios between the number concentrations of each fraction and the overall mean number concentration for each year we get the relative contribution of each fraction from the overall particle count. This comparison (Figure 7) then shows that the years 2018 and 2019 were almost identical in terms of the ratios between the average number concentrations of the individual fractions.

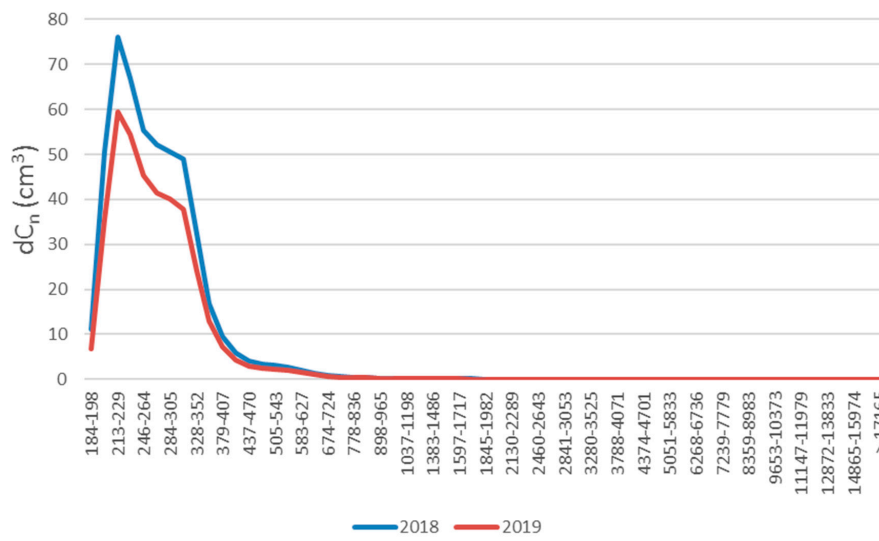


Figure 6. Comparison between average number concentration for all size fractions for 2018 and 2019.

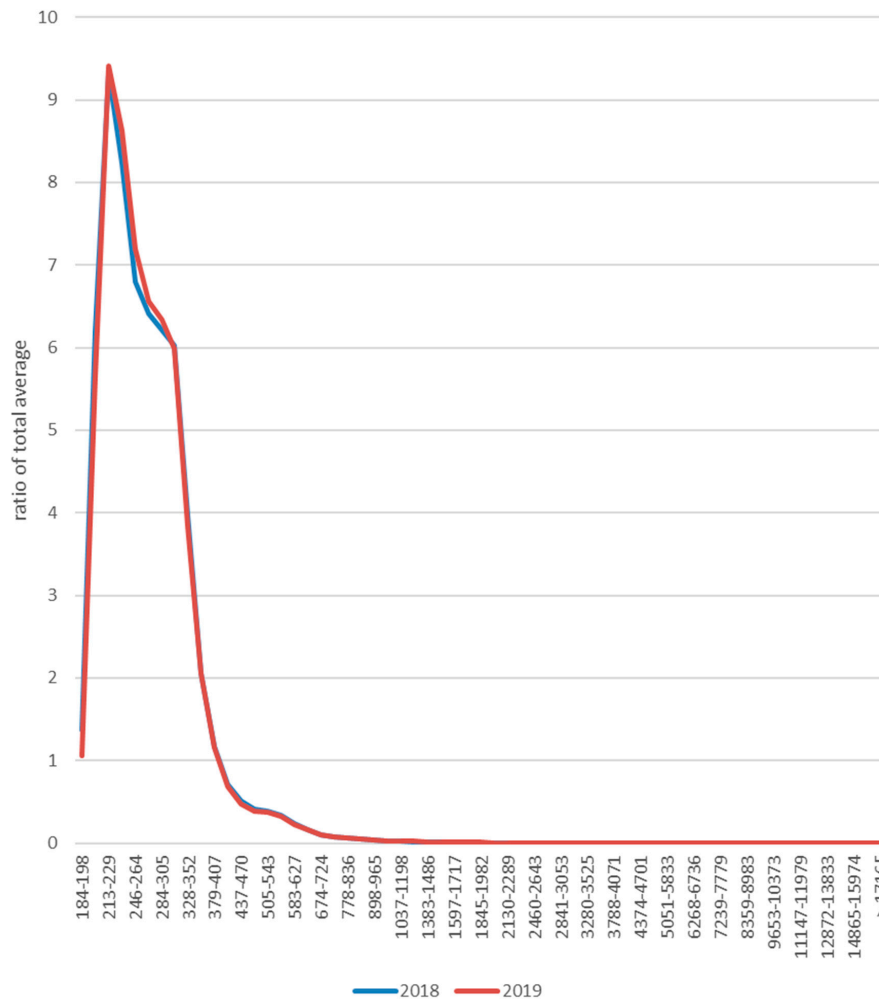


Figure 7. Comparison between the contribution of each average number concentration to the overall total for 2018 and 2019.

4. Discussion

The results of the analysis proved that the annual and daily variation in number concentrations can differ a lot in relation to the particle size. It has been shown that in the case of smaller particles in the range from approximately 200 to 800 nm, there is a significant variability throughout the year, with much higher values, particularly in the winter months. This is most likely due to the variability in particle sources during the year. In cold conditions, the intensity of heating increases significantly (being almost negligible in summer months) and local domestic heating becomes a very significant source of air pollution. Even though traffic is a very important suspended particles source at this location, it is a stable source in that it is relevant both in the summer and in the winter (although meteorological and dispersion conditions [34–36], which are in general worse in the winter – lower wind speed, less precipitation, temperature inversions – can lead to a higher number of particles in the air in winter months).

Higher number concentrations in the winter months compared to the warm months were observed especially in the case of the PM₁ particles. Larger particles did not show such a trend. This is in accordance with other studies. For example Vecchi [17] observed an increase of PM₁ in the winter period by a factor of 2.5 compared to the summer, while in the case of PM_{2.5} the increase was only by a factor of approximately 2. A similar conclusion was also made in a study by Triantafyllou et al. [37], which showed a more significant increase of smaller particles in the winter period.

The most significant difference between the winter and summer period has been observed for particles in the range between 300 and 800 nm. Particles of this size can be a product of heating. Zhang et al. [38] analyzed emissions from coal combustion. They concluded that while primary particles generated by coal combustion have a size of approximately 10 to 30 nm, their subsequent coagulation leads to the formation of particles approximately 500 nm large, which is in accordance with the findings of this study.

Apart from heating, low temperature also affects traffic exhaust emissions. This was proved for example by a study by Weilenmanna et al. [39], which showed that a vehicle cold start has a significant negative effect especially on the emissions of CO and HC, but to a lesser extent also suspended particles.

Larger particles show higher number concentrations in the warm period of the year. This could be due to the fact that combustion generally produces smaller particles and some sources of larger particles are significant especially in the warm part of the year. This includes for example resuspension, which is more significant in the summer than in the winter when the surface is cold and soil frozen [40]. Traffic is a significant contributor to resuspension.

When looking at the differences in daily variation of the individual fractions it is obvious that there is a much more significant difference between day and night in the case of the larger particles, which show higher number concentrations during the day. The number of larger particles increases in the morning, in correlation with the morning traffic peak. Vehicles can produce these larger particles by resuspension or abrasion of brake pads, clutch, tires, and the road surface. Number concentration falls significantly in the evening. This is most likely due to the higher mass of these particles, which are therefore more likely to deposit on the ground.

In contrast, the number concentrations of the smaller particles do not differ between day and night to such an extent as the larger particles. As Figure 2 shows, two peaks can also be seen, corresponding to the morning and afternoon traffic peak, but the average number concentration of day and night do not differ as much.

The minimum number concentration is observed around noon and early afternoon hours, not during the night. This is in accordance with other studies focusing on this topic. A study by Zhu [41] showed that even though the traffic intensity at night is 75% lower than during the day, the number of submicron particles only dropped by 20%. Explanation of this could be that the wind speed at night is lower and another possible answer is that there is a weaker atmospheric dilution at night. One other factor is air temperature. Air temperature is on average lower at night and colder ambient temperatures contribute to significantly increased nuclei mode particle formation in vehicle

exhaust [42,43]. Pérez et al. [44] think that the reason for higher concentrations of smaller particles at night compared to the larger ones could also be the decrease of the boundary layer height. Lower air temperature and higher air relative humidity are a favorable factor for condensation and coagulation processes between particles and precursor gases [45].

5. Conclusions

In this study, an analysis of number concentrations in 61 size fractions of suspended particles was made focusing on the difference in daily and annual variation. Data comes from ambient air quality monitoring station Ústí nad Labem-Všebořická, an urban traffic station, with data available from mid-June 2017 to the end of 2019.

The results of the study showed that there are significant differences in both the annual and daily number concentration variations depending on the particle size. In the case of the annual variation, a higher variability can be seen for the smaller particles (Figure 4). This is most likely related to the sources of these particles. The most significant source of PM_{2.5} particles in the Czech Republic is local domestic heating. This source, however, is almost negligible in the summer months. In contrast, in the case of the daily variation there is a higher variability of the larger particles (Figure 2). This can be explained by the fact that these larger particles deposit quicker to the ground and also by meteorological conditions as explained in the paper. Given that the most significant source of suspended particles at this station is traffic, there are obvious peaks in suspended particle concentrations correlating with morning peak hour and afternoon peak hour. In the evening and at night, there is a rapid decrease in the number of large particles in the air. Smaller particles do not deposit to such an extent so their number concentration remains higher at night. Additionally, a comparison was made between number concentrations on weekdays (Monday-Friday) and weekends (Saturday-Sunday), when the traffic intensity is much lower. The comparison showed that in this case, the variation is very similar to the daily variation in that there is a much more obvious decrease of larger particles number concentrations (Figure 3).

Meteorological and dispersion conditions have a very important effect on air quality. Their variability can cause very significant differences from year to year in terms of absolute values of number concentrations. A comparison between 2018 and 2019, however, showed that the relative ratio between the number concentrations of the various size fractions remain very similar (Figure 7).

It can be concluded that the differences in variation between the various size fractions are determined by both the actual pollution sources (especially in the long-term, i.e., annual variation) and by the actual physical properties of the particles and their behavior in the atmosphere, also determined by the meteorological and dispersion conditions.

In the future, it would be ideal to research annual and daily variation of different size fractions at more station types, i.e., not just traffic stations, but also suburban and rural background stations and also repeat the analysis when a longer time-series is available.

Author Contributions: Conceptualization, V.A. and J.B.; methodology, J.B. and V.A.; formal analysis, K.K.; investigation, V.A., J.B. and K.K.; resources, J.B. and K.K.; data curation, J.B.; writing—original draft preparation, J.B. and K.K.; writing—review and editing, K.K.; visualization, J.B.; supervision, V.A.; project administration, K.K.; funding acquisition, J.B. All authors have read and agreed to the published version of the manuscript.

Funding: This paper is supported by the Czech Hydrometeorological Institute.

Conflicts of Interest: The authors declare no conflict of interest.

References

1. World Health Organization. *Ambient Air Pollution—a Major Threat to Health and Climate*; World Health Organization: Copenhagen, Denmark, 2018.
2. Loxham, M.; Davies, D.E.; Holgate, S.T. The health effects of fine particulate air pollution. *BMJ* **2019**. [[CrossRef](#)]
3. Zhang, Y.L.; Cao, F. Fine particulate matter (PM_{2.5}) in China at a city level. *Sci. Rep.* **2015**, *5*, 14884. [[CrossRef](#)]

4. Kim, K.H.; Kabir, E.; Kabir, S. A review on the human health impact of airborne particulate matter. *Environ. Int.* **2015**, *74*, 136–143. [[CrossRef](#)] [[PubMed](#)]
5. Luo, X.; Bing, H.; Luo, Z.; Wang, Y.; Jin, L. Impacts of atmospheric particulate matter pollution on environmental biogeochemistry of trace metals in soil-plant system: A review. *Environ. Pollut.* **2019**, *255*. [[CrossRef](#)] [[PubMed](#)]
6. Banerjee, T.; Kumar, M.; Singh, N. *Aerosol, Climate, and Sustainability. Encyclopedia of the Anthropocene*; Elsevier: Oxford, UK, 2018; pp. 419–442. ISBN 9780128135761. [[CrossRef](#)]
7. Zhu, Y.; Hinds, W.C.; Shen, S.; Sioutas, C. Seasonal Trends of Concentration and Size Distribution of Ultrafine Particles Near Major Highways in Los Angeles Special Issue of Aerosol Science and Technology on Findings from the Fine Particulate Matter Supersites Program. *Aerosol Sci. Technol.* **2004**, *38* (Suppl. 1), 5–13. [[CrossRef](#)]
8. Baldauf, R.W.; Devlin, R.B.; Gehr, P.; Giannelli, R.; Hassett-Sipple, B.; Jung, H.; Narubum, G.; McDonald, J.; Sacks, J.D.; Walker, K. Ultrafine Particle Metrics and Research Considerations: Review of the 2015 UFP Workshop. *Int. J. Environ. Res. Public Health* **2016**, *13*, 1054. [[CrossRef](#)] [[PubMed](#)]
9. Zhao, Y.; Nalwa, H.S. (Eds.) *Nanotoxicology: Interactions of Nanomaterials with Biological Systems*; American Scientific Publishers: Los Angeles, CA, USA, 2007.
10. Chen, L.Q.; Fang, L.; Ling, J.; Ding, C.Z.; Kang, B.; Huang, C.Z. Nanotoxicity of silver nanoparticles to red blood cells: Size dependent adsorption, uptake, and hemolytic activity. *Chem. Res. Toxicol.* **2015**, *28*, 501–509. [[CrossRef](#)]
11. Gehrig, R.; Brigitte, B. Characterising seasonal variations and spatial distribution of ambient PM10 and PM2.5 concentrations based on long-term Swiss monitoring data. *Atmos. Environ.* **2003**, *37*, 2571–2580. [[CrossRef](#)]
12. Li, J.; Chen, B.; de la Campa, A.M.S.; Alastuey, A.; Querol, X.; Jesus, D. 2005–2014 trends of PM10 source contributions in an industrialized area of southern Spain. *Environ. Pollut.* **2018**, *236*, 570–579. [[CrossRef](#)]
13. Bartzis, J.G.; Kalimeri, K.K.; Sakellaris, I.A. Environmental data treatment to support exposure studies: The statistical behavior for NO2, O3, PM10 and PM2.5 air concentrations in Europe. *Environ. Res.* **2020**, *181*. [[CrossRef](#)]
14. Samek, L.; Stegowski, Z.; Styszko, K.; Furman, L.; Fiedor, J. Seasonal contribution of assessed sources to submicron and fine particulate matter in a Central European urban area. *Environ. Pollut.* **2018**, *241*, 406–411. [[CrossRef](#)] [[PubMed](#)]
15. Křůmal, K.; Mikuška, P.; Vojtěšek, M.; Večeřa, Z. Seasonal variations of monosaccharide anhydrides in PM1 and PM2.5 aerosol in urban areas. *Atmos. Environ.* **2010**, *44*, 5148–5155. [[CrossRef](#)]
16. Asimakopoulou, D.N.; Maggos, T.; Assimakopoulou, V.D.; Bougiatioti, A.; Bairachtari, K.; Vasilakos, C.; Mihalopoulos, N. Chemical characterization, sources and potential health risk of PM2.5 and PM1 pollution across the Greater Athens Area. *Chemosphere* **2020**, *241*. [[CrossRef](#)]
17. Vecchi, R.; Marazzan, G.; Valli, G.; Ceriani, M.; Antoniazzi, C. The role of atmospheric dispersion in the seasonal variation of PM1 and PM2.5 concentration and composition in the urban area of Milan (Italy). *Atmos. Environ.* **2004**, *38*, 4437–4446. [[CrossRef](#)]
18. Samek, L.; Furman, L.; Mikrut, M.; Regiel-Futyra, A.; Macyk, W.; Stochel, G.; van Eldik, R. Chemical composition of submicron and fine particulate matter collected in Krakow, Poland. Consequences for the APARIC project. *Chemosphere* **2017**, *187*, 430–439. [[CrossRef](#)]
19. Gugamsetty, B.; Wei, H.; Liu, C.N.; Awasthi, A.; Hsu, S.C.; Tsai, C.J.; Roam, G.D.; Wu, Y.C.; Chen, C.F. Source Characterization and Apportionment of PM10, PM2.5 and PM0.1 by Using Positive Matrix Factorization. *Aerosol Air Qual. Res.* **2012**, *12*, 476–491. [[CrossRef](#)]
20. Carbone, C.; Decesari, S.; Paglione, M.; Giulianelli, L.; Rinaldi, M.; Marinoni, A.; Cristofanelli, P.; Didiodato, A.; Bonasoni, P.; Fuzzi, S.; et al. 3-year chemical composition of free tropospheric PM1 at the Mt. Cimone GAW global station—South Europe—2165 m a.s.l. *Atmos. Environ.* **2014**, *87*, 218–227. [[CrossRef](#)]
21. Spindler, G.; Grüner, A.; Müller, K.; Schlimper, S.; Herrmann, H. Long-term size-segregated particle (PM10, PM2.5, PM1) characterization study at Melpitz—Influence of air mass inflow, weather conditions and season. *J. Atmos. Chem.* **2013**, *70*, 165–195. [[CrossRef](#)]
22. Pitz, M.; Kreyling, W.G.; Hölscher, B.; Cyrus, J.; Wichmann, H.E.; Heinrich, J. Change of the ambient particle size distribution in East Germany between 1993 and 1999. *Atmos. Environ.* **2001**, *35*, 4357–4366. [[CrossRef](#)]
23. Liu, Y.; Fu, B.; Shen, Y.; Yu, Y.; Liu, H.; Zhao, Z.; Zhang, L. Seasonal properties on PM1 and PGEs (Rh, Pd, and Pt) in PM1. *Atmos. Pollut. Res.* **2018**, *9*, 1032–1037. [[CrossRef](#)]

24. Titos, G.; Lyamani, H.; Pandolfi, M.; Alastuey, A.; Alados-Arboledas, L. Identification of fine (PM1) and coarse (PM10-1) sources of particulate matter in an urban environment. *Atmos. Environ.* **2014**, *48*, 593–602. [[CrossRef](#)]
25. Tao, J.; Shen, Z.; Zhu, C.; Yue, J.; Cao, J.; Liu, S.; Zhu, L.; Zhang, R. Seasonal variations and chemical characteristics of sub-micrometer particles (PM1) in Guangzhou, China. *Atmos. Res.* **2012**, *118*, 222–231. [[CrossRef](#)]
26. Pinto, J.A.; Kumar, P.; Alonso, M.F.; Andreão, W.L.; Pedruzzi, R.; dos Santos, F.S.; Moreira, D.M.; de Almeida Albuquerque, T.T. Traffic data in air quality modeling: A review of key variables, improvements in results, open problems and challenges in current research. *Atmos. Pollut. Res.* **2020**, *11*, 454–468. [[CrossRef](#)]
27. Hu, D.; Wu, J.; Tian, K.; Liao, L.; Xu, M.; Du, Y. Urban air quality, meteorology and traffic linkages: Evidence from a sixteen-day particulate matter pollution event in December 2015, Beijing. *J. Environ. Sci.* **2017**, *59*, 30–38. [[CrossRef](#)] [[PubMed](#)]
28. Dėdėlė, A.; Miškinytė, A. Seasonal and site-specific variation in particulate matter pollution in Lithuania. *Atmos. Pollut. Res.* **2019**, *10*, 768–775. [[CrossRef](#)]
29. Kamińska, J.A. The use of random forests in modelling short-term air pollution effects based on traffic and meteorological conditions: A case study in Wrocław. *J. Environ. Manag.* **2018**, *217*, 164–174. [[CrossRef](#)] [[PubMed](#)]
30. Zhang, Z.; Zhang, X.; Gong, D.; Quan, W.; Zhao, X.; Ma, Z.; Kim, S.J. Evolution of surface O₃ and PM_{2.5} concentrations and their relationships with meteorological conditions over the last decade in Beijing. *Atmos. Environ.* **2015**, *108*, 67–75. [[CrossRef](#)]
31. Laña, I.; Del Ser, J.; Padró, A.; Vélez, M.; Casanova-Mateo, C. The role of local urban traffic and meteorological conditions in air pollution: A data-based case study in Madrid, Spain. *Atmos. Environ.* **2016**, *145*, 424–438. [[CrossRef](#)]
32. Google Maps Steetview. (28.4.2020). Ústí nad Labem. Available online: <https://goo.gl/maps/inqx7S1vjV94w1DdA> (accessed on 18 May 2020).
33. Seznam. Mapy.cz. (28.4.2020). Ústí nad Labem. Available online: <https://en.mapy.cz/s/kubonunano> (accessed on 18 May 2020).
34. Ramsey, N.R.; Klein, P.M.; Moore, B., III. The impact of meteorological parameters on urban air quality. *Atmos. Environ.* **2014**, *86*, 58–67. [[CrossRef](#)]
35. Fisher, B. Meteorological factors influencing the occurrence of air pollution episodes involving chimney plumes. *Meteorol. Appl.* **2002**, *9*, 199–210. [[CrossRef](#)]
36. Radaideh, J.A. Effect of Meteorological Variables on Air Pollutants Variation in Arid Climates. *J. Environ. Anal. Toxicol.* **2017**, *7*. [[CrossRef](#)]
37. Triantafyllou, E.; Diapouli, E.; Korras-Carraca, M.B.; Manousakas, M.; Psanis, C.; Floutsi, A.A.; Spyrou, C.; Eleftheriadis, K.; Biskos, G. Contribution of locally-produced and transported air pollution to particulate matter in a small insular coastal city. *Atmos. Pollut. Res.* **2020**, *11*, 667–678. [[CrossRef](#)]
38. Zhang, L.; Ninomiya, Y.; Yamashita, T. Formation of submicron particulate matter (PM1) during coal combustion and influence of reaction temperature. *Fuel* **2006**, *85*, 1446–1457. [[CrossRef](#)]
39. Weilenmann, M.; Favez, J.Y.; Alvarez, R. Cold-start emissions of modern passenger cars at different low ambient temperatures and their evolution over vehicle legislation categories. *Atmos. Environ.* **2009**, *43*, 2419–2429. [[CrossRef](#)]
40. Keramat, A.; Marivani, B.; Samsami, M. Climatic Change, Drought and Dust Crisis in Iran. *World Academy of Science. Environ. Eng.* **2011**, *6*, 10–13. [[CrossRef](#)]
41. Zhu, Y.; Kuhn, T.; Mayo, P.; Hinds, W.C.; HINDS. Comparison of Daytime and Nighttime Concentration Profiles and Size Distributions of Ultrafine Particles near a Major Highway. *Environ. Sci. Technol.* **2006**, *40*, 2531–2536. [[CrossRef](#)] [[PubMed](#)]
42. Wei, Q.; Kittelson, D.B.; Watts, W.F. Single-Stage Dilution Tunnel Performance. SAE Transaction: Warrendale, PA, USA, 2001. [[CrossRef](#)]
43. Kittelson, D.; Johnson, J.; Watts, W.; Wei, Q.; Drayton, M.; Paulsen, D.; Bukowiecki, N. Diesel Aerosol Sampling in the Atmosphere. In *SAE Transactions Journal of Fuels and Lubricants*; SAE Paper No. 2000-01-2212; SAE: Warrendale, PA, USA, 2000.

44. Pérez, N.; Pey, J.; Cusack, M.; Reche, C.; Querol, X.; Alastuey, A.; Viana, M. Variability of Particle Number, Black Carbon, and PM 10, PM 2.5, and PM 1 Levels and Speciation: Influence of Road Traffic Emissions on Urban Air Quality. *Aerosol Sci. Technol.* **2010**, *44*, 487–499. [[CrossRef](#)]
45. Jamriska, M.; Morawska, L.; Mergersen, K. The effect of temperature and humidity on size segregated traffic exhaust particle emissions. *Atmos. Environ.* **2008**, *42*, 2369–2382. [[CrossRef](#)]



© 2020 by the authors. Licensee MDPI, Basel, Switzerland. This article is an open access article distributed under the terms and conditions of the Creative Commons Attribution (CC BY) license (<http://creativecommons.org/licenses/by/4.0/>).